JOURNAL OF COMPUTATIONAL PHYSICS 104, 277–284 (1993)

NOTE

On the Numerical Solution of the Cubic Schrödinger Equation in One Space Variable

1. INTRODUCTION

Despite numerous numerical studies of the cubic nonlinear Schrödinger equation, many questions remain open. In this note, we return to basic issues involving the time and spatial discretizations of the equation defined over the entire real line. Two spatial discretizations are considered, the L^2-Galerkin method with product approximation and the integrable finite difference scheme of Ablowitz and Ladik [1]. The nonlinear implicit system of ordinary differential equations (ODEs) arising from the L^2-Galerkin spatial discretization is solved by the code D02NNF, an ODE solver from the NAG library. The use of D02NNF surmounts numerous difficulties encountered by commonly used time-stepping schemes. It is shown that the Galerkin method suffers from an instability during long time integrations with features similar to those observed for the periodic problem. This instability may be avoided by using the integrable finite difference scheme, with the time integration performed by the NAG ODE solver D02NCF. However, the integrable scheme appears to be more susceptible to phase errors than the L^2-Galerkin method.

The ubiquitous nonlinear Schrödinger (NLS) equation is given by

$$iu_t + u_{xx} + q\,|u|^2 u = 0, \quad (x, t) \in (-\infty, \infty) \times (0, T], \tag{1a}$$

$$u(x, 0) = g(x), \quad x \in (-\infty, \infty), \tag{1b}$$

where $i^2 = -1$; $u(x, t)$ and the given function $g(x)$ are complex-valued. We shall only consider the focusing case, that is, we assume q to be a positive constant. Appropriate initial conditions include the case where $|g(x)| \to 0$ as $|x| \to \infty$, which we call the infinite line problem, and also the periodic case where $g(x + L) = g(x)$. Physically, the equation arises in a number of situations. In general, it describes the envelope solutions of weakly nonlinear dispersive systems; see, for example, Newell [12]. We note that (1a) is the dimensionless form of the equation. Since the pioneering work of Zakharov and Shabat [20], it has been shown that the NLS equation has a truly remarkable analytical structure; see, for example, Ablowitz and Segur [2]. For our purposes, it is sufficient to note that it can be viewed as a completely integrable, infinite dimensional Hamiltonian system with Hamiltonian

$$H = \int (|u_x|^2 - \tfrac{1}{2} q\,|u|^4)\,dx. \tag{2a}$$

A second integral invariant that is of interest is the squared L^2 norm

$$C = \int |u|^2\,dx. \tag{2b}$$

The integrals in (2) are over the interval $(-\infty, \infty)$ or over one spatial period. These constants are two of an infinite number that are strongly connected to the integrability of the equation.

Some of the other remarkable features associated with the NLS equation include soliton solutions in the infinite line problem and homoclinic orbits in the periodic case; see Ercolani *et al.* [6]. These features, combined with the fact that explicit analytical solutions are often available, have given rise to much interest in the NLS equation among numerical analysts. For example, associated with the homoclinic orbits of the periodic problem is a sensitivity to small perturbations. This may lead to numerical instabilities and even spurious numerical chaos; see [8, 9]. One way of avoiding this problem is to design integrable discretizations that preserve the qualitative structure of the phase space of the analytical problem. This leads to significant improvements whenever one attempts to calculate a solution in the sensitive area near a homoclinic orbit.

Interesting numerical issues also arise in the infinite line problem. For instance, a bound state of two or more solitons develops steep temporal and spatial gradients, which present a challenge for most numerical schemes. Since these problems are defined over the entire real line, one has either to truncate the infinite interval or to introduce a mapping from it to a finite interval that can be handled numerically. Weideman and Cloot [19] have shown that careful attention to the question of boundary conditions

0021-9991/93 $5.00

may significantly improve the quality and efficiency of the numerical approximation.

In this note, we are interested in basic questions regarding the temporal and spatial discretizations of the infinite line problem. In order to simplify the discussion, we do not address any of the issues involving the boundary conditions. Instead, we sacrifice efficiency by moving the boundaries far enough out so that they do not interfere with the solution in the interior. Accordingly, we restrict x to a finite interval $[a, b]$, chosen so that the modulus of the solution $u(x, t)$ is negligible for x outside $[a, b]$. Homogeneous Neumann (or Dirichlet) boundary conditions are imposed at $x = a$ and $x = b$, thereby converting the pure initial value problem (1) into an initial boundary-value problem (IBVP). If the interval $[a, b]$ is sufficiently large, the choice of Neumann or Dirichlet boundary conditions is not critical, and as a consequence we consider the IBVP

$$iu_t + u_{xx} + q|u|^2 u = 0, \quad (x, t) \in (a, b) \times (0, T], \tag{3a}$$

$$u(x, 0) = g(x), \quad x \in (a, b), \tag{3b}$$

$$u_x(a, t) = u_x(b, t) = 0, \quad t \in [0, T], \tag{3c}$$

which is, in fact, the case most often examined in the literature.

Several previous numerical studies have examined the use of finite difference methods and finite element methods based on the L^2-Galerkin semi-discretization for solving IBVPs of this form; see, for example, [7, 10, 14–17, 5, 18], the case of homogeneous Dirichlet boundary conditions being considered in the last two studies. On the other hand, the integrable scheme of Ablowitz and Ladik [1] has received comparatively little attention in the numerical analysis literature, despite the fact that it is eminently suited for numerical calculations. Its main advantage is that, as one would expect of an integrable scheme, it does not suffer from nonlinear instabilities, unlike the standard numerical methods. Although the integrable scheme captures the qualities of the analytical solutions, it remains a second-order approximation. In fact, we find that it suffers from phase errors that are more severe than those of some of the standard schemes of comparable accuracy.

Methods for the time discretization have received much attention in the literature. However, none of the time stepping schemes considered in previous studies has proved to be entirely satisfactory for both the computation of the modulus of the approximate solution and the determination of approximations to the two conserved quantities C and H. The situation is further complicated by the fact that the linearized problem

$$u_t = iu_{xx}$$

has all of its eigenvalues on the imaginary axis. A time stepping scheme with this property, such as the leapfrog scheme, therefore seems to be appropriate. However, it has been shown to suffer from blowup instabilities in the nonlinear situation; see, for example, Sanz-Serna and Verwer [16]. This indicates that one should consider schemes that include the imaginary axis in their regions of stability. This excludes the higher order backward differentiation formulas underlying the stiff systems solvers in the software libraries such as NAG. An inspection of their stability regions reveals that for problems with all eigenvalues on the imaginary axis, the backward differentiation formulas are stable provided the time step is large enough. However, this does not take nonlinear effects into account and an examination of the use of state-of-the-art software, specifically the codes D02NNF and D02NCF, ODE solvers from the NAG library which implement backward differentiation formulas, for the solution of the systems of nonlinear ordinary differential equations arising from the semi-discretizations of (3), shows that these codes offer substantial improvement over commonly used time-stepping schemes. Codes from the NAG library were chosen for use in this study because of the wide availibility of this library. One would expect software of similar quality to perform in a comparable fashion.

2. BACKGROUND

2.1. The Test Problems

In our study we consider the solution of the NLS in the case of a bound state of solitons. This class of problems poses a stringent test of numerical schemes due to the steep spatial and temporal gradients encountered. The L^2-Galerkin scheme with product approximation has been successfully employed for the solution of two simpler classes of test problems, that of a single soliton (a traveling wave) and the interaction of two solitons (two colliding waves); see, for example, [7, 10, 13, 17, 18]. Extensive numerical experiments using the L^2-Galerkin method with product approximation and D02NNF for the solution of these classes of problems were presented in [13].

The bound state of multiple solitons is a class of problems in which the initial condition is

$$g(x) = \operatorname{sech}(x) \tag{4}$$

and $q = 2L^2$ for L a positive integer. In this case, the conserved quantities in (2) have the values

$$H = \tfrac{2}{3}(1 - q), \quad C = 2, \tag{5}$$

respectively. The theoretical solution for a bound state of solitons is well known; see [11], for example. However, the solution is not at present in a usable form if $L \geqslant 3$.

2.2. The Numerical Methods

2.2.1. *Spatial Discretization*

The L^2-Galerkin spatial discretization applied to the IBVP (3) was described by Griffiths *et al.* [7] and Herbst *et al.* [10]. In each of these studies, the solution u of (3) is approximated by

$$U(x, t) = \sum_{j=0}^{N} U_j(t)\, \xi_j(x), \tag{6}$$

where $\{\xi_j\}_{j=0}^{N}$ is the usual basis for the space of continuous piecewise linear functions defined on a uniform grid with spacing $h = (b-a)/N$. When product approximation [4] is employed, the functions $U_j(t) = V_j(t) + iW_j(t)$ are defined by

$$M\dot{\mathbf{U}} + h^{-2}S\mathbf{U} + qM\mathbf{F}(\mathbf{U}) = \mathbf{0}, \tag{7}$$

where the dot denotes differentiation with respect to time,

$$\mathbf{U} = [V_0, W_0, ..., V_N, W_N]^{\mathrm{T}},$$
$$\mathbf{F} = [\mathbf{F}_0, ..., \mathbf{F}_N]^{\mathrm{T}},$$
$$\mathbf{F}_j = [W_j(V_j^2 + W_j^2), -V_j(V_j^2 + W_j^2)],$$

and M and S are the block tridiagonal matrices

$$M = \tfrac{1}{6} J_1 \otimes I, \quad S = J_2 \otimes \hat{I},$$

with $\otimes$ denoting the matrix tensor product,

$$J_1 = \begin{pmatrix} 2 & 1 & & & & & \\ 1 & 4 & 1 & & & & \\ & \ddots & \ddots & \ddots & & & \\ & & \ddots & \ddots & \ddots & & \\ & & & \ddots & \ddots & \ddots & \\ & & & & 1 & 4 & 1 \\ & & & & & 1 & 2 \end{pmatrix},$$

$$J_2 = \begin{pmatrix} -1 & 1 & & & & & \\ 1 & -2 & 1 & & & & \\ & \ddots & \ddots & \ddots & & & \\ & & \ddots & \ddots & \ddots & & \\ & & & \ddots & \ddots & \ddots & \\ & & & & 1 & -2 & 1 \\ & & & & & 1 & -1 \end{pmatrix},$$

I is the 2×2 identity, and

$$\hat{I} = \begin{pmatrix} 0 & 1 \\ -1 & 0 \end{pmatrix}.$$

In practice we have found that entirely satisfactory results are obtained when the initial approximation $U(x, 0)$ is determined by interpolating the initial data, in which case

$$U_j(0) = g(a + jh), \quad j = 0, 1, ..., N.$$

The second scheme which we consider is the integrable finite difference scheme of Ablowitz and Ladik [1],

$$i\dot{U}_j + (U_{j-1} - 2U_j + U_{j+1})/h^2 + \tfrac{1}{2} q\, |U_j|^2 (U_{j-1} + U_{j+1}) = 0. \tag{8}$$

From its infinite number of conservation laws we single out the two corresponding to C and H, namely,

$$C_a = h \sum_j U_j^* U_{j-1} \tag{9a}$$

and

$$H_a = h^{-3} \sum_j [-h^2 U_j^* (U_{j-1} + U_{j+1}) + 4q^{-1} \ln(1 + \tfrac{1}{2} h^2 q U_j U_j^*)], \tag{9b}$$

where * denotes complex conjugation. Note that the Hamiltonian (9b) of the Ablowitz–Ladik scheme is a non-obvious discretization of the analytical one. It should also be pointed out that it has nonstandard Poisson brackets although this fact is of no consequence in our present study.

2.2.2. *Time Discretization*

The system (7) is solved using D02NNF, a general purpose routine for integrating the initial value problem (IVP) for a stiff system of *implicit* differential equations coupled with algebraic equations of the form

$$A(t, \mathbf{y})\dot{\mathbf{y}} = \mathbf{g}(t, \mathbf{y});$$

see [3]. The time stepping is done using a backward differentiation formula integrator. The *explicit* system (8) is solved using D02NCF, a routine for integrating stiff systems of explicit ODEs when the Jacobian is a banded matrix [3]. As in D02NNF, the time stepping is performed by a backward differentiation formula integrator.

2.2.3. *Previous Studies*

We now summarize several previous numerical studies involving the case of a bound state of solitons. Herbst *et al.* [10] examined (3) with the initial condition given by (4) and $q = 2L^2$, for L a positive integer. Since problems similar to the $q = 2$ case, a bound state of a single soliton, were handled without difficulty in earlier studies (see, for

example, [7, 15]), Herbst *et al.* concentrated on the $q = 8$ and $q = 18$ cases, and, for the spatial discretization, they used the L^2-Galerkin method (7). Herbst *et al.* derived analogues of the conservation laws associated with (2) (for the continuous-time Galerkin approximation U) when the L^2-Galerkin method is used without product approximation. When product approximation is employed, these laws are no longer satisfied. However, the authors claimed that discrete analogues of the conservation laws obtained using the trapezoidal rule to approximate the integrals are satisfied when "mass lumping" is applied to yield a finite difference scheme. Herbst *et al.* then utilized the implicit midpoint rule and a modification of it due to Delfour *et al.* [5] for the time discretization. In their numerical experiments, Herbst *et al.* found that the $q = 8$ case presented no difficulties but they encountered significant challenges when $q = 18$. With either time-stepping scheme, the results obtained using the L^2-Galerkin space discretization were superior to those arising from the mass lumping. However, even in the L^2-Galerkin results, the graph of $|U|$ exhibited noticeable deviations from the time-periodic behavior of $|u|$, and the approximations to H were not conserved to even a single significant figure. The appearance of undesirable downstream oscillations was another recurring problem.

Sanz-Serna and Verwer [16] considered a standard finite difference scheme for the space discretization for the $q = 18$ case and applied two time discretizations, the implicit midpoint rule and a "pseudolinear" midpoint rule. For sufficiently small mesh spacings in both space and time ($h = 0.03125$, with $\Delta t = 0.00625$ for the former and $\Delta t = 0.003125$ for the latter), both methods integrated the problem successfully. No approximations to the conserved quantities were presented.

Sanz-Serna and Christie [14] also considered the $q = 18$ case, using a finite difference scheme for the space discretization and the implicit midpoint rule for the time discretization. They utilized adaptive mesh selection procedures in both space and time. No three-dimensional graphs of $|U|$ and no values of approximations to the conserved quantities C and H were presented. However, a cross section of the graph of $|U|$ at $t = 0.98$ was produced which was in close agreement with a cross section of the graph of $|U|$ at the same value of t obtained using a uniform spatial grid with $h = 0.03125$.

More recently, Shamardan [17] considered several test problems, including a bound state of three solitons, using a fourth-order finite difference discretization in space and the implicit midpoint rule for the time integration. The utilization of this approach with $h = 0.0625$ and $\Delta t = 0.01$ produced an approximation to $C^{1/2}$ which was perfectly conserved and which agreed with $C^{1/2}$ to seven decimal places. However, the graph of the modulus of the approximate solution had a non-symmetric appearance at $t = 2.5$.

3. NUMERICAL EXPERIMENTS

All computations were performed on the University of Kentucky's IBM 3090-600J in double precision using its vectorization facilities. The graphs were produced using SAS/GRAPH.

3.1. Time Discretization

Once the initial approximation $\mathbf{U}(0)$ has been determined, the IVP (7) is solved using the NAG routine D02NNF. Prior to calling D02NNF, calls are made to the appropriate linear algebra setup routine and integrator setup routine. Because of the structure of the coefficient matrices and the nature of the function $\mathbf{F}$, the Jacobian in the L^2-Galerkin method is considered as banded with upper and lower bandwidth 3, and the linear algebra setup routine D02NTF is used. The NAG routine D02NCF is employed for the solution of the explicit system (8). The integrator setup routine used throughout this study is D02NVF, which implements the BDF (backward differentiation formula) integrator. In our numerical experiments we use a uniform grid in the x-direction with spacing $h = (b - a)/N$, as was done in most of the previous studies. When using the L^2-Galerkin method with product approximation, the graph of $|U|$, the modulus of the approximate solution, is obtained along with graphs of C' and H', approximations to the two conserved quantities C, H, respectively, where C' and H' are computed exactly using three-point Gauss quadrature on each subinterval to evaluate the integrals

$$\int_a^b |U|^2 \, dx, \quad \int_a^b (|U_x|^2 - \tfrac{1}{2} q |U|^4) \, dx,$$

respectively. For comparison purposes the quantities C and H, given by (5), are graphed on the same set of axes as C' and H'. Similarly, when using the integrable finite difference scheme, C and H are graphed on the same set of axes as C_a and H_a. Throughout this study, the maximum order of the BDF integrator is set at 5, which provides us with entirely satisfactory results. The quantities RTOL and ATOL, tolerances used in a mixed relative and absolute local error test in D02NNF, are set at $\text{RTOL} = 10^{-5}$ and $\text{ATOL} = 10^{-8}$.

3.2. Numerical Results

3.2.1. *Bound State of Three Solitons*

We first consider the case of a bound state of three solitions, solving the problem using the L^2-Galerkin method with product approximation and D02NNF. More extensive numerical experiments using this approach on the same test problem were given in [13].

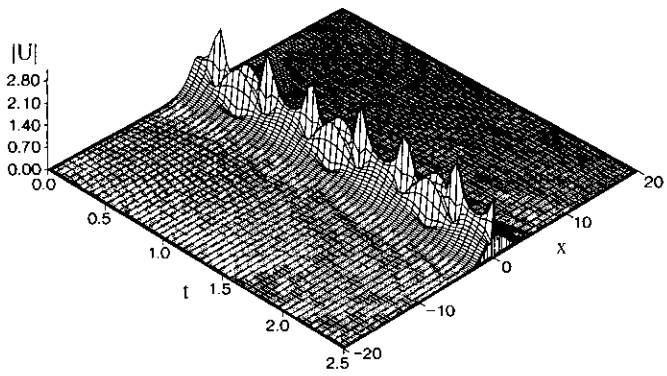

FIG. 1. Bound state of three solitons, L^2-Galerkin method, $N = 640$: graph of $|U|$.

The spatial interval used is $[-20, 20]$, as in previous studies. In all experiments involving this test problem, the quantities C' and H' are computed and the graph of $|U|$ is drawn at

$$t_j = 0.05j, \quad j = 1, 2, ..., 50.$$

At each point (x_k, t_j), where the x_k are 201 uniformly spaced points, $|U|$ is calculated from (6). The graphical package then constructs the graph by connecting these points by straight lines.

In this problem, the solution is time-periodic; the graph of the modulus rises from the initial condition of $|g(x)| = \operatorname{sech}(x)$ to reach a spike, followed by a pair of symmetric ridges, followed by a second spike, and then returns to its initial shape to begin another period, a period being approximately 0.8 units. The use of $N = 320$ produces an approximate solution whose graph is seriously in error after approximately the first period. Increasing N to 640 produces a satisfactory graph (Fig. 1). Some wave activity is nonetheless apparent away from the central spine. The same phenomenon was observed in Figs. 4–10 of [10], where it

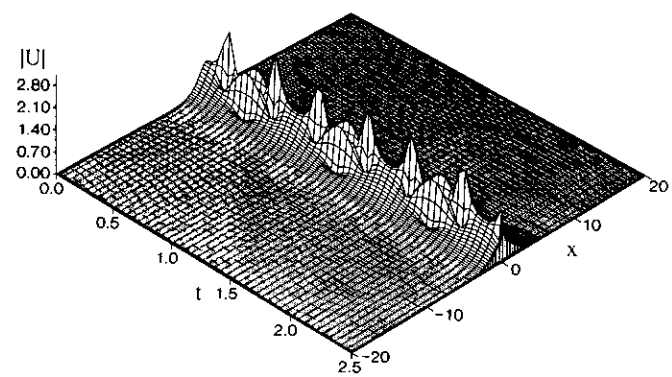

FIG. 2. Bound state of three solitons, L^2-Galerkin method, $N = 1280$: graph of $|U|$.

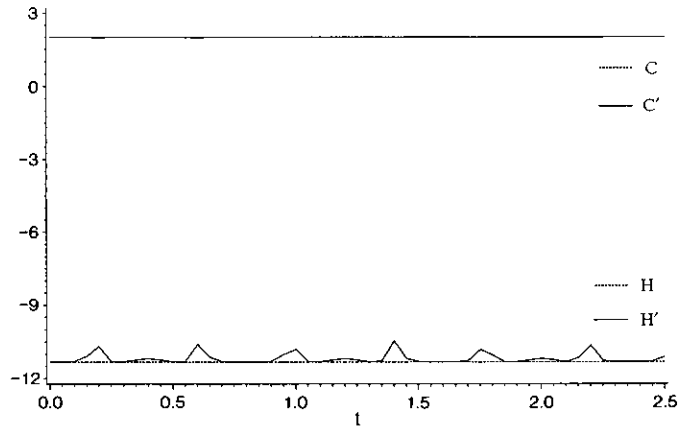

FIG. 3. Bound state of three solitons, L^2-Galerkin method, $N = 640$: graphs of conserved quantities and approximations.

was referred to as "leaking (of) energy." Figure 2 is obtained with 1280 subintervals. The wave activity has been eliminated, and other differences between this graph and Fig. 1 are slight. Comparing the graphs, we can see that increasing N retards the propagation of the numerical solution over time, with the result that the graph of $|U|$ comes closer to exhibiting the correct time-periodic behavior. Also, the cross section of the graph of the modulus at $t = 2.5$ is perfectly symmetric about $x = 0$, unlike the graph in [17]. As can be seen from Figs. 3 and 4, C' is always in close agreement with C, while the behavior of H' improves considerably as N is increased.

The graph in Fig. 4 of [16] was produced using a finite difference spatial discretization with $N = 1280$ and the implicit midpoint rule for the time-stepping. The periodic behavior is observed throughout, with the seventh spike just beginning to form at $t = 2.5$. Figure 2 of the present study exhibits the correct behavior. In Figs. 9 and 10 of [10], which were obtained using the L^2-Galerkin method and

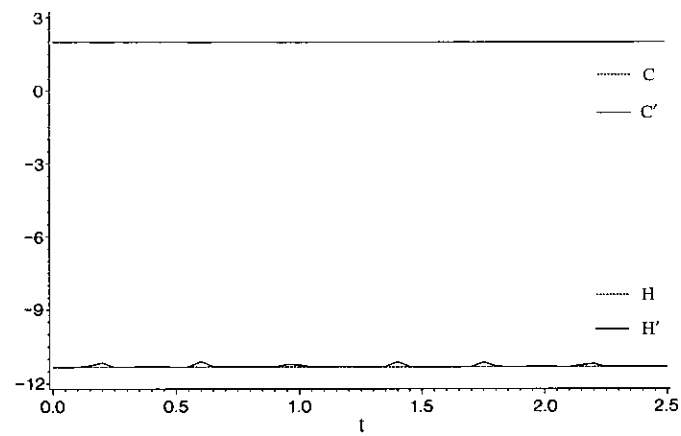

FIG. 4. Bound state of three solitons, L^2-Galerkin method, $N = 1280$: graphs of conserved quantities and approximations.

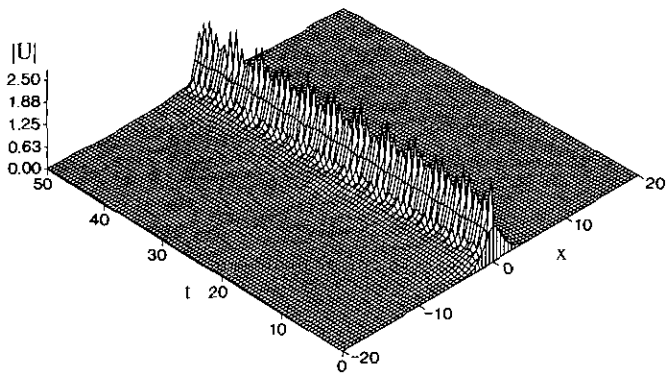

FIG. 5. Bound state of two solitons, integrable scheme, $N = 80$: graph of $|U|$.

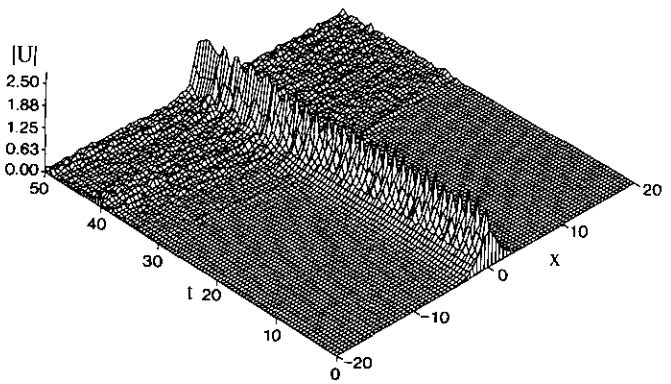

FIG. 7. Bound state of two solitons, L^2-Galerkin method, $N = 80$: graph of $|U|$.

product approximation with $N = 400$ and the midpoint rule and modified midpoint rule, respectively, for the time discretization, the seventh spike has already occurred by $t = 2.5$. Herbst *et al.* indicated that their approximation to H was not conserved to even a single significant digit when $N = 400$.

By sufficiently increasing the value of N, we are able to obtain results which are an improvement on those presented by Herbst *et al.*, who indicated that a further reduction in h and Δt did not produce significant changes in their solutions. Since the only difference between our L^2-Galerkin method and that of Herbst *et al.* is in the time-stepping, it would appear that the use of D02NNF is the source of the improvement. By increasing N to 1280, Sanz-Serna and Verwer were able to produce a graph of $|U|$ of comparable quality to those we have obtained, but they did not present any values of approximations to the two conserved quantities, C and H.

3.2.2. *Long Time Integrations and the Integrable Scheme*

In the case of a bound state of solitons, most of the numerical experiments reported in the literature as well as the experiments discussed so far in this paper have been restricted to integrating over fairly short time intervals. We now investigate what happens in long time integrations. In particular, we are interested in a comparison between the L^2-Galerkin method and the integrable finite difference scheme of Ablowitz and Ladik. The test problem is the bound state of two solitons, i.e., $q = 8$ with the initial condition (4). The spatial interval is again taken to be $[-20, 20]$ and a uniform mesh spacing with $h = 0.5$ is employed. We compute up to $t = 50$, graphing $|U|$ every 0.5 units of time and plotting the solution at the grid points.

The graph of the modulus of the approximate solution obtained using the integrable scheme is shown in Fig. 5. A comparison with the graph of the modulus of the theoretical solution (Fig. 6) shows that the integrable scheme suffers from phase errors. Although the solution is qualitatively correct, it does not produce the proper number of peaks over the interval of integration. While the integrable scheme maintains the qualitative behavior of the solution over this long time integration, the Galerkin scheme suddenly develops an instability in the form of a corruption of the

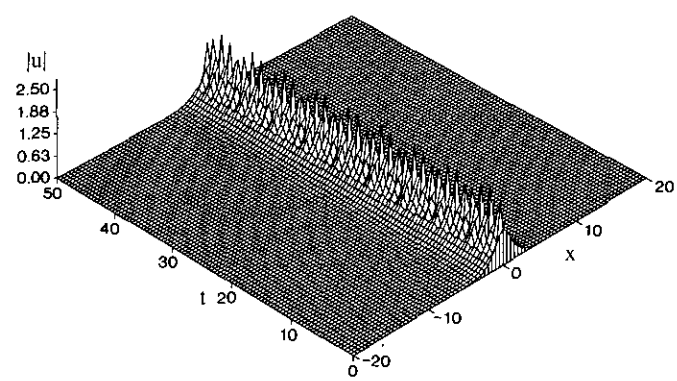

FIG. 6. Bound state of two solitons: graph of modulus of theoretical solution.

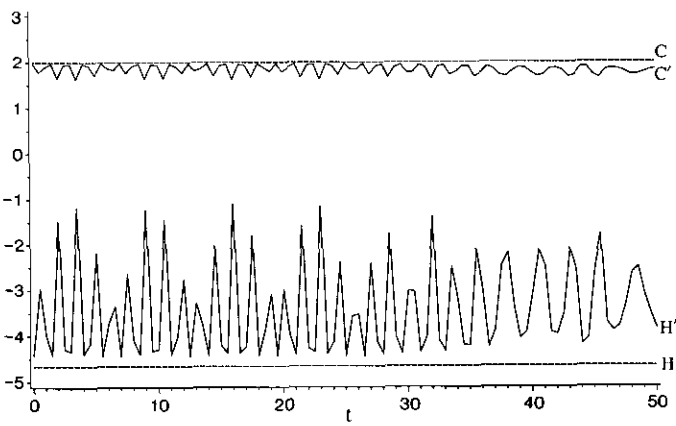

FIG. 8. Bound state of two solitons, L^2-Galerkin method, $N = 80$: graphs of conserved quantities and approximations.

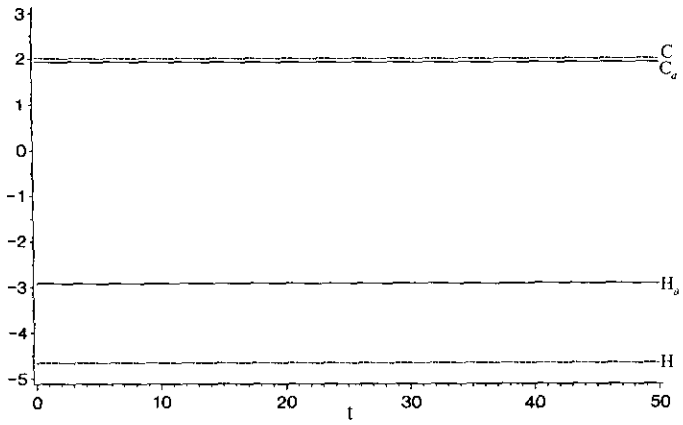

FIG. 9. Bound state of two solitons, integrable scheme, $N = 80$: graphs of conserved quantities and approximations.

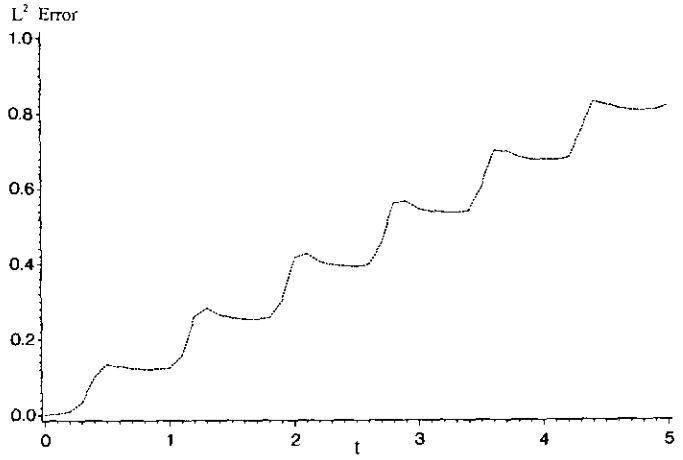

FIG. 11. Bound state of two solitons, L^2-Galerkin method, $N = 320$: L^2 error.

spatial structure by high frequency components, cf. Fig. 7. Prior to the appearance of this instability, the Galerkin scheme is more accurate than the integrable scheme.

Note that the instability develops with little or no warning. A similar situation has been encountered in the periodic problem. There, the instability consists of two components—homoclinic crossings and a corruption of the spatial structure. The latter is very similar to what we observe in Fig. 7. In the periodic case, the instability is traced to the double points in the nonlinear spectrum of the associated eigenvalue problem. In the present problem, defined over the whole real line, the high frequency components observed in the spatial structure correspond to activating the continuous spectrum of the associated linear eigenvalue problem. An investigation of the origins of the instability in the infinite line case is beyond the scope of this work.

The behavior of the approximations to the conserved quantities C and H is also informative. The quantities C' and H' computed from the Galerkin solution exhibit noticeable oscillations, corresponding to the spikes in the graph of $|U|$ (Fig. 8). These variations become somewhat less pronounced once the instability appears around $t = 30$, but after this has occurred, C' and H' do not approach C and H at subsequent times. On the other hand, C_a and H_a, computed from the solution obtained using the integrable scheme, are well conserved (Fig. 9). However, they differ from the values of C and H. In numerical experiments conducted with the integrable scheme over shorter time intervals, we have observed that $C_a \to C$ and $H_a \to H$ as $h \to 0$.

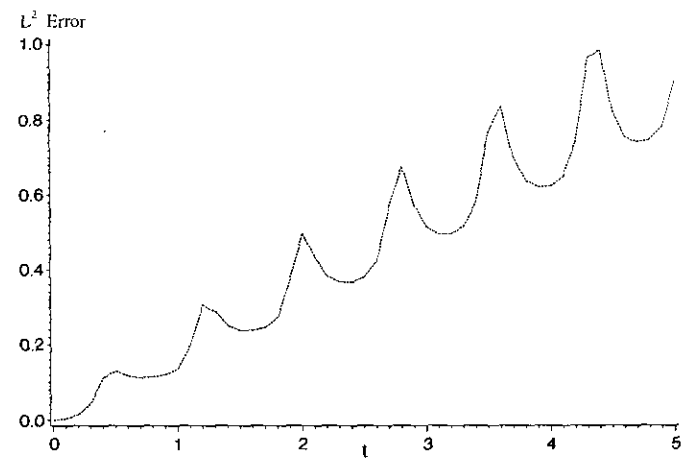

FIG. 10. Bound state of two solitons, integrable scheme, $N = 320$: L^2 error.

As a final observation, we note that when either method is employed, the L^2 error displays a "staircase" behavior with increasing t, at least until phase errors or instabilities intervene. This is illustrated by the graphs in Figs. 10 and 11, produced, respectively, using the integrable scheme (with D02NCF) and the Galerkin scheme (with D02NNF) and solving the problem on $[-20, 20] \times [0, 5]$ with $h = 0.125$ and output every 0.1 units of time. In each case, the periodic jumps in the L^2 error correspond to the appearance of spikes in the graph of $|U|$.

4. CONCLUDING REMARKS

The results of numerical experiments demonstrate the efficacy of the NAG routine D02NNF. For example, in the case of a bound state of three solitons, we obtain a graph of $|U|$ which is comparable to the best one presented in [16] and of higher accuracy than those presented in [10, 17]. The conservation laws are no longer satisfied by the L^2-Galerkin semi-discretization when product approximation is employed. Nevertheless, we have obtained values of approximations to the two quantities C and H which are approximately constant and, in many instances, substantial improvements over those previously presented. When the

exact values C and H are known, the values of the approximations to these two quantities obtained in our experiments are in close agreement with them.

We have also identified an instability in long time integrations that we expect to observe with many of the standard, nonintegrable space discretizations during long-time integrations. This is clearly a nonlinear instability and a detailed study of this phenomenon involves the structure of its associated nonlinear spectrum and is beyond the scope of the present investigation. However, we have demonstrated that the instability may be avoided using the integrable discretization of Ablowitz and Ladik. On the other hand, this scheme appears to be more susceptible to phase errors than the L^2-Galerkin scheme. Also, integrable schemes are designed specifically for individual problems and more general numerical techniques remain as important as ever.

ACKNOWLEDGMENTS

We thank Bernard Bialecki, Karin Bennett, and Ryan Fernandes of the University of Kentucky for their assistance during the preparation of this paper, and Ian Gladwell of Southern Methodist University for valuable advice during the initial phases of this investigation. This research was supported in part by funds from the National Science Foundation Grant RII-8610671 and the Commonwealth of Kentucky through the University of Kentucky's Center for Computational Sciences.

REFERENCES

1. M. J. Ablowitz and J. F. Ladik, *Stud. Appl. Math.* **55**, 213 (1976).
2. M. J. Ablowitz and H. Segur, *Solitons and the Inverse Scattering Transform* (SIAM, Philadelphia, 1981).
3. M. Berzins, R. W. Brankin, and I. Gladwell, Numerical Analysis Report 143, Dept. of Mathematics, University of Manchester, 1987.
4. I. Christie, D. F. Griffiths, A. R. Mitchell, and J. M. Sanz-Serna, *IMA J. Numer. Anal.* **1**, 253 (1981).
5. M. Delfour, M. Fortin, and G. Payre, *J. Comput. Phys.* **44**, 277 (1981).
6. N. Ercolani, M. G. Forest, and D. W. McLaughlin, *Physica D*, to appear.
7. D. F. Griffiths, A. R. Mitchell, and J. Ll. Morris, *Comput. Methods Appl. Mech. Eng.* **45**, 177 (1984).
8. B. M. Herbst and M. J. Ablowitz, *Phys. Rev. Lett.* **62**, 2065 (1989).
9. B. M. Herbst and M. J. Ablowitz, in *Integrable Systems and Applications*, edited by M. Balabane, P. Lochak, and C. Sulem, Lecture Notes in Physics, Vol. 342 (Springer-Verlag, Berlin, 1989).
10. B. M. Herbst, J. Ll. Morris, and A. R. Mitchell, *J. Comput. Phys.* **60**, 282 (1985).
11. J. W. Miles, *SIAM J. Appl. Math.* **41**, 227 (1981).
12. A. C. Newell, *Solitons in Mathematics and Physics* (SIAM, Philadelphia, 1985).
13. M. Robinson and G. Fairweather, Technical Report CCS-89-4, University of Kentucky Center for Computational Sciences, Lexington, Kentucky, 1989.
14. J. M. Sanz-Serna and I. Christie, *J. Comput. Phys.* **67**, 348 (1986).
15. J. M. Sanz-Serna and V. S. Manoranjan, *J. Comput. Phys.* **52**, 273 (1983).
16. J. M. Sanz-Serna and J. G. Verwer, *IMA J. Numer. Anal.* **6**, 25 (1986).
17. A. B. Shamardan, *Comput. Math. Appl.* **19**, 67 (1990).
18. Y. Tourigny and J. Ll. Morris, *J. Comput. Phys.* **76**, 103 (1988).
19. J. A. C. Weideman and A. Cloot, *Comput. Methods Appl. Mech. Eng.* **80**, 467 (1990).
20. V. E. Zakharov and A. B. Shabat, *Sov. Phys. JETP* **34**, 62 (1972).

Received November 1, 1990; revised October 18, 1991

M. P. ROBINSON

Department of Mathematics
Western Kentucky University
Bowling Green, Kentucky 42101

G. FAIRWEATHER

Departments of Mathematics
and Engineering Mechanics
University of Kentucky
Lexington, Kentucky 40506

B. M. HERBST

Department of Applied Mathematics
University of the Orange Free State
Bloemfontein 9300
Republic of South Africa